An Adaptive Neuro-Fuzzy Inference System-Based Approach for Oil and Gas Pipeline Defect Depth Estimation

Abduljalil Mohamed*, Mohamed Salah Hamdi*, and Sofiène Tahar**
* Ahmed Bin Mohamed Military College/Information Systems Department, Doha, Qatar
** Concordia University/Electrical and Computer Engineering Department, Montreal, Quebec, Canada
{ajmaoham, mshamdi}@abmmc.edu.qa, tahar@ece.concordia.ca

***Abstract*—To determine the severity of metal-loss defects in oil and gas pipelines, the depth of potential defects, along with their length, needs first to be estimated. For this purpose, pipeline engineers use intelligent Magnetic Flux Leakage (MFL) sensors that scan the metal pipelines and collect defect-related data. However, due to the huge amount of the collected MFL data, the defect depth estimation task is cumbersome, time-consuming, and error-prone. In this paper, we propose an adaptive neuro-fuzzy inference system (ANFIS)-based approach to estimate defect depths from MFL signals. Depth-related features are first extracted from the MFL signals and then are used to train the neural network to tune the parameters of the membership functions of the fuzzy inference system. A hybrid learning algorithm that combines least-squares and back propagation gradient descent method is adopted. Moreover, to achieve an optimal performance by the proposed approach, highly-discriminant features are selected from the obtained features by using the weight-based support vector machine (SVM). Experimental work has shown that encouraging results are obtained. Within error-tolerance ranges of ±15%, ±20%, ±25%, and ±30%, the depth estimation accuracies obtained by the proposed technique are 80.39%, 87.75%, 91.18%, and 95.59%, respectively. Moreover, further improvement can be easily achieved by incorporating new and more discriminant features.**

Keywords—Neural networks; fuzzy inference systems; adaptive learning; feature extraction; feature selection

I. INTRODUCTION

Because gas and oil production is carried through long-distance transmission metallic pipelines, nearly 30% of underground or underwater pipeline defects is caused by external corrosion [1]. The consequences of these defects to the environment and human life are immeasurable. Thus, an advanced intelligent system that can monitor these pipelines and determine the severity of potential metal-loss defects is urgently required. The majority of techniques reported in the literature utilize Magnetic Flux Leakage (MFL) signals and ultrasonic waves to detect and localize defect types such as corrosion, dents, cracks, etc. MFL signals behave differently when they are recorded around the center of a metal-loss defect. The closer the sensors measuring MFL signals to the defect center, the higher is the amplitude of the axial and radial components of the MFL signals. For sensors that are further away from the defect center, the measured amplitude of the abovementioned components gets lower. Thus, neighborhood sensors could play a crucial role in determining the type and size of a defect. Techniques reported in the literature rely heavily on MFL signals. In [2], a fuzzy-neural network-based approach is proposed for reliability assessment of oil and gas pipelines. The actual condition of corroded pipelines is characterized by eight parameters obtained from MFL signals. These parameters in turn are used for training a probabilistic neural network. The probability of defect failure can then be estimated using the trained neural network. An automatic inspection system for pipeline surface defects is proposed in [3]. As a preprocessing step, it uses image processing techniques to analyze scanned images of pipes in order to extract crack-related features. In the classification step, a neuro-fuzzy algorithm is applied such that membership functions learn variations of feature values. The proposed technique shows a good classification accuracy. The authors of [4] propose an artificial neural networks-based pattern recognition system. It classifies acquired MLF signals into three types of defects in the weld joint of pipelines. These defects are external corrosion (EC), internal corrosion (IC), and lack of penetration (LP), and are intentionally inserted in the weld bead of a pipeline. The reported results show that ANNs were able to correctly classify signals with non-defect (ND) and signals with defects (D) along the weld bead with high accuracy at 94.2%. For signals that represent the defects LP and corrosion (CO), the classification accuracy obtained was 92.2%. In [5], the authors propose a Radial Basis Function Neural Network (RBFNN) to recognize and quantify corrosion characteristics in a pipeline. To obtain training data for the neural network, several corrosion spots were artificially made on the pipeline and MFL data were collected. The Immune RBFNN (IRBFNN) algorithm processed the MFL data to determine the location and size of the corrosion spots. The proposed method successfully identified the location and size of corrosion in the pipe.

The relationship between the amplitude of the MFL signal and the depth of the corresponding defect is not well-understood. As a result, an analytical model that accurately describes this relationship is not available. Therefore, intelligent tools such as Adaptive Neuro-Fuzzy Inference Systems (ANFIS) can be used to learn this relationship. To the best of our knowledge, ANFIS have never been used to estimate metal-loss defect depths. In this paper, defect depth-

978-1-4673-7606-8/15/$31.00 ©2015 IEEE

related features are first extracted from MFL signals that represent different defect shapes. The discriminant qualities of these features are examined by a weight correlation scheme. Based on these weights, a subset of features is selected to train the Sugeno-fuzzy system; a hybrid learning algorithm that comprises of least-squares and backpropagation gradient descent method is used in the training stage [6].

The rest of the paper is organized as follows. In Section II, we review the techniques used in detecting and locating pipeline defects. The proposed ANFIS-based defect depth estimation approach is introduced in Section III. In Section IV, the performance evaluation of the proposed approach is described. We conclude with final remarks in Section V.

II. MFL-Based Pipeline Inspection

A. MFL Signals

Autonomous devices, equipped with strong magnets and magnetic sensors and used as nondestructive inspection tools, are called intelligent pigs. The essential role of these devices is to utilize a pipe scanning technique and measure any *magnetic flux leakage* within the pipes. An intelligent pig is sent into and retrieved from the pipes. The sensors that are equally-distributed around the pipeline circumference move with the intelligent pig parallel to the axis of the pipeline. The concept of MFL scanning is as follows [7]: The surface of a pipeline gets magnetized when two strong magnets of opposite polarity are held close to it. Magnetic flux (lines of magnetic force) flow through the walls of the pipeline from the south Pole to the north pole. If the wall of the pipeline contains a crack or a thinning (due to corrosion, for example), at the edges of the crack two new poles appear. The air gap between the two new edges, however, cannot absorb as much flux per unit of magnetic flux as the ferromagnetic material. This causes the magnetic lines of force to bulge out. The bulging triggers the MFL signals. Leakage of magnetic flux is an indication of the presence of a defect. These MFL signals are later analyzed to locate possible defects and determine their sizes and severity levels.

B. Wavelet-based Techniques for Pipeline Defect Detection and Sizing

In this work, wavelet techniques can be used to locate and estimate the length of metal-loss defects. Since they are a powerful mathematical tool [8, 9, 10], wavelet techniques have been successfully applied in other problem domains such as high-efficiency data compression [11], data analysis and classification [12], and efficient de-noising [13, 14, 15]. In [16], they are used for detecting metal-loss defects. In addition to locate a metal-loss defect, pattern-adapted wavelets can also be used for estimating defect-length as MFL signals take a certain shape at the location of a metal-loss defect. The defect shape occurs in a dilated form. A sample MFL scan signal, denoted by B, is shown in Fig. 1. The signal contains three defects of cuboidal shape. The three components of the MFL signal (B_x, B_y, and B_z) are represented. Each of these components consists of a sum of curves, and is a translated and dilated version of a reference pattern. Let a mother wavelet $\psi(x)$ refer to the reference pattern, and $\langle \psi_{j,k}(x) \rangle$ to an orthonormal wavelet basis, then the MFL $B(x)$ can be described as expressed in the basis as:

$$B(x) = \sum_{j,k} c_{j,k} \psi_{j,k}(x), \quad (1)$$

The coefficients $c_{j,k}$ are non-zero and indicate the signal contains a copy of that particular instance $\psi_{j,k}(x)$. When the wavelet transform of the MFL scan $B(x)$ is computed with respect to the basis $\langle \psi_{j,k}(x) \rangle$, the set of non-zero coefficients indicate the locations of metal-loss defects along the pipeline. Moreover, the set of dilation factors of the reference pattern is determined, which yields the widths of the defects.

III. ANFIS-Based Defect Depth Estimation Model

ANFIS have been successfully used in different application areas such as water quality management [17], queue management [18], energy [19], transportation [20, 21], and business and manufacturing [22, 23, 24, 25]. In this section, the applicability of ANFIS models in estimating metal-loss defect depth is demonstrated. The general architecture of the proposed approach is shown in Fig. 2.

A. Feature Extraction and Selection

To reduce data dimensionality, discriminant features are first extracted from the raw MFL signals. Representative features that characterize the original MFL signals can lead to a better performance for the ANFIS model and reduce the training session. The following features are extracted:

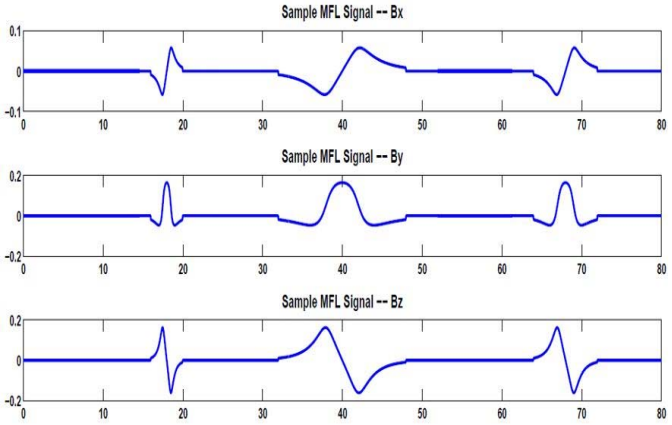

Fig. 1. Sample MFL scan of a pipeline with three metal-loss defects of cuboidal shape

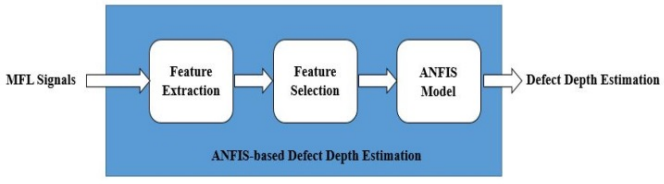

Fig. 2. The structure diagram of the proposed approach

978-1-4673-7606-8/15/$31.00 ©2015 IEEE

- Maximum magnitude
- Peak-to-peak distance
- Integral of the normalized signal
- Mean average
- Standard deviation

Moreover, MFL signals can be approximated by polynomial series of the form, $a_n X^n + ... + a_1 X + a_0$. Polynomials of degrees 3, 6, and 6 have been found to provide the best approximation for B_x , B_y and B_z , respectively. Thus, the input feature consists of the polynomial coefficients, $a_n + ... + a_0$, along with the above features. Thus, in total we have 33 features, which will be referred to by F1, F2… and F33.

Often, incorporating all obtained features in the training process may not lead to a high depth estimation accuracy. In fact, including some features may have a negative impact. Therefore, it is a common practice to identify the important features that are appropriate to the ANFSI model.

B. Architecture of ANFIS

Jang [6] introduced the idea of ANFIS in 1993, which is basically a fuzzy inference system implemented in the framework of adaptive networks. It maps inputs through input membership functions (MFs) to outputs through output membership functions. Domain knowledge can be used to design the initial membership functions and rules for the fuzzy inference system. It is shown in [6] that even if such knowledge is not available, the adaptive neuro-fuzzy inference system can generate the set of fuzzy *if-then* rules that approximate a desired set of input-output data pairs. As shown in Fig. 3, the ANFIS structure consists of five layers, where each layer consist of several nodes described by node functions. The outputs of the neurons of each layer present the inputs for the succeeding layer.

The parameters of the adaptive nodes, shown as square nodes in Fig. 3, are adjustable, whereas the parameters of the fixed nodes, shown as circle nodes in the figure, are fixed. To explain the procedure of the ANFIS, we consider two inputs *x*, *y*, one output *f*, and one degree of Sugeno's function that depicts the fuzzy rule in the fuzzy inference system [6]. Thus, two fuzzy *if-then* rules will be contained in the rule base as follows:

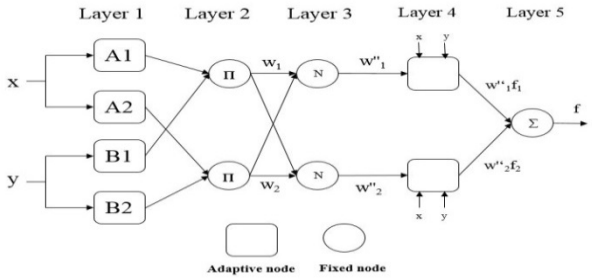

Fig. 3. The architecture of ANFIS

Rule 1: if x is A_1 and y is B_1 then $f = p_1 x + q_1 y + r_1$.

Rule 2: if x is A_2 and y is B_2 then $f = p_2 x + q_2 y + r_2$.

where p_i, q_i, r_i are adaptable parameters. The node functions in each layer is described in the sequel.

Layer 1: Each node in this layer is an adaptive node and is given as follows:

$$o_i^1 = \mu_{Ai}(x), \qquad i = 1,2 \tag{2}$$

$$o_i^1 = \mu_{Bi-2}(y), \qquad i = 3,4 \tag{3}$$

Where x and y are inputs to the layer nodes, and A_i , B_{i-2} are linguistic variables. The maximum and minimum of the bell-shaped membership function are 1 and 0, respectively. The membership function has the following form:

$$\mu_{Ai}(x) = \frac{1}{1 + \{(\frac{x - c_i}{a_i})^2\}^{bi}} \tag{4}$$

Where the set $\{a_i, b_i, c_i\}$ represents the premise parameters of the membership function. The bell-shaped function changes according to the change of values in these parameters.

Layer 2: Each node in this layer is a fixed node. Its output is the product of the two input signals as follows:

$$o_i^2 = w_i = \mu_{Ai}(x)\mu_{Bi}(y), \qquad i = 1,2 \tag{5}$$

Where w_i refers to the firing strength of a rule.

Layer 3: Each node in this layer is a fixed node. Its function is to normalize the firing strength as follows:

$$o_i^3 = w_i^{"} = \frac{w_i}{w_1 + w_2}, \qquad i = 1,2 \tag{6}$$

Layer 4: Each node in this layer is adaptive and adjusted as follows:

$$o_i^4 = w_i^{"} f_i = w_i^{"}(p_i x + q_i y + r_i), \quad i = 1,2 \tag{7}$$

Where $w_i^{"}$ is the output of layer 3 and $\{p_i + q_i + r_i\}$ is the consequent parameter set.

Layer 5: Each node in this layer is fixed and computes their outputs as follows:

$$o_i^5 = \sum_{i=1}^{2} w_i^{"} f_i = \frac{(\sum_{i=1}^{2} w_i f_i)}{w_1 + w_2} \tag{8}$$

The output of layer 5 sums the outputs of nodes in layer 4 to be the output of the whole network. If the parameters of the premise part are fixed, the output of the whole network will be the linear combination of the consequent parameters, i.e.,

$$f = \frac{w_1}{w_1 + w_2} f_1 + \frac{w_2}{w_1 + w_2} f_2 \tag{9}$$

978-1-4673-7606-8/15/$31.00 ©2015 IEEE

The adopted training technique is hybrid, in which, the network node outputs go forward till layer 4, and the resulting parameters are identified by the least square method. The error signal, however, goes backward till layer 1, and the premise parameters are updated according to the descent gradient method. It has been shown in the literature that the hybrid-learning technique can obtain the optimal premise and consequent parameters in the learning process [6].

C. Learning Algorithm for ANFIS

To map the input/output data set, the adaptable parameters $\{a_i + b_i + c_i\}$ and $\{p_i + q_i + r_i\}$ in the ANFIS structure are adjusted in the learning process. When the premise parameters a_i, b_i and c_i of the membership function are fixed, the ANFIS yields the following output as shown in (9). Substituting (6) into (9), we obtain the following:

$$f = w_1^{"} f_1 + w_2^{"} f_2 \tag{10}$$

Substituting the fuzzy *if-then* rules in (10) yields:

$$f = w_1^{"}(p_1 x + q_1 y + r_1) + w_2^{"}(p_2 x + q_2 y + r_2) \tag{11}$$

or:

$$f = (w_1^{"} x) p_1 + (w_1^{"} y) q_1 + (w_1^{"}) r_1) + (w_2^{"} x) p_2 + (w_2^{"} y) q_2 + (w_2^{"}) r_2 \tag{12}$$

Equation (12) is a linear combination of the adjustable parameters. The optimal values of $\{a_i, b_i, c_i\}$ and $\{p_i, q_i, r_i\}$ can be obtained by using the least squared method. If the premise parameters are fixed, the hybrid learning algorithm can effectively search for the optimal ANFIS parameters.

IV. Performance Evaluation

In this section, the applicability of the neuro-fuzzy computing techniques for defect depth estimation in oil and gas pipelines is evaluated. Extensive experimental work has been conducted. The evaluation of the ANFIS model will be mainly based on the estimation accuracy of the defect depth within a certain level of error-tolerance as required by industry standards. The error-tolerance levels used in this study are ±1%, ±5%, ±10%, ±15%, ±20%, ±25%, ±30%, ±35%, and ±40%. The ANFIS model is tested on different combinations of extracted features. The results are reported in the following subsections.

A. Membership Functions of Input Features

A membership function (MF) is the curve that defines how each point in the universe of discourse of a given feature is mapped to a membership value between 0 and 1. The membership value indicates the degree to which the relevant input feature belongs to a certain metal-loss defect depth. The Gaussian curve membership seems to be appropriate for the extracted features. As shown in Fig. 4, only two parameters are needed to determine the function shape for each input feature, namely the standard deviation and mean.

B. Training of the ANFIS Model

In this experimental work, we consider only 29 features of the 33 abovementioned features. Four features, namely, F3, F6, F8, and F13 are excluded because their values were not acceptable by the ANFIS model (their learned sigma values were very close to zero). There are 1357 data samples that are used for the developing and testing the ANFIS model. These data samples are divided into 70% for training, 15% for testing, and 15% for checking. The training data set consists of 949 rows and 30 columns. The rows represent the training samples, and the first 29 columns represent the extracted features of each sample and the last column represents the target (defect depth). The format of the testing and checking data is similar to the training, however, each consists of 204 rows (samples). We have used 100 epochs to train the ANFIS model. The hybrid learning approach is adopted, in which the membership function parameters of single-out Sugeno type fuzzy inference system are identified. The hybrid learning approach converges much faster than the original backpropagation method. In the forward pass, the node outputs go forward until layer 4 and the consequent parameters are identified with the least square method. In the backward pass, the error rates propagate backward and the premise parameters are updated by gradient decent.

C. Single Feature-based ANFIS Model

To determine the estimation quality for each input feature, the ANFIS model is first trained and examined using individual features. The results for each single feature are shown in Tables I, II, and III. It should be noted from these tables that different features yield different defect depth estimation accuracies. Seven features, however, present the best estimation accuracy among all features, namely F1, F4, F9, F10, F11, F14, and F32. Consequently, we examine the ANFIS model on these selected features.

TABLE I. Defect Depth Estimation Accuracy of the Anfis Model for F1- F14 Features with Different Error-Tolearnce

Error-Tolerance	Input Parameters				
	F1	F2	F4	F5	F7
±1%	0.0196	0.0196	0.0147	0.0049	0.0441
±5%	0.1176	0.0980	0.1275	0.1029	0.1127
±10%	0.2892	0.1520	0.2990	0.1765	0.2108
±15%	0.4510	0.2647	0.4755	0.2353	0.2647
±20%	0.6275	0.3382	0.6471	0.3235	0.3627
±25%	0.8137	0.4216	0.8039	0.3971	0.4363
±30%	0.8775	0.4951	0.8971	0.5098	0.5490
±35%	0.9265	0.6029	0.9314	0.5980	0.6225
±40%	0.9461	0.6863	0.9510	0.7059	0.7059

Error-Tolerance	Input Parameters				
	F9	F10	F11	F12	F14
±1%	0.0294	0.0490	0.0196	0	0.0147
±5%	0.1618	0.1176	0.1373	0.0931	0.1618
±10%	0.3627	0.2304	0.3235	0.2010	0.2941
±15%	0.5637	0.4118	0.4902	0.2647	0.5000
±20%	0.7549	0.5686	0.6667	0.3333	0.6618
±25%	0.9265	0.6912	0.8137	0.4216	0.8578
±30%	0.9461	0.7990	0.9020	0.5343	0.9167
±35%	0.9510	0.9020	0.9412	0.6029	0.9363
±40%	0.9559	0.9314	0.9559	0.6814	0.9461

978-1-4673-7606-8/15/$31.00 ©2015 IEEE

TABLE II. DEFECT DEPTH ESTIMATION ACCURACY OF THE ANFIS MODEL FOR F15- F24 FEATURES WITH DIFFERENT ERROR-TOLEARNCE

Error-Tolerance	Input Parameters				
	F15	F16	F17	F18	F19
±1%	0.0147	0.0196	0.0245	0.0098	0.0049
±5%	0.1029	0.1127	0.1029	0.1078	0.1078
±10%	0.1863	0.1912	0.1961	0.2108	0.1814
±15%	0.2451	0.2500	0.3186	0.2500	0.2402
±20%	0.3333	0.3431	0.4118	0.3578	0.3431
±25%	0.3873	0.4461	0.5392	0.4461	0.4265
±30%	0.5098	0.5588	0.5882	0.5343	0.5049
±35%	0.6078	0.6176	0.7010	0.6373	0.6275
±40%	0.7059	0.7108	0.7647	0.7206	0.7206

Error-Tolerance	Input Parameters				
	F20	F21	F22	F23	F24
±1%	0.0098	0.0098	0.0294	0.0098	0.0294
±5%	0.0931	0.0686	0.0735	0.1029	0.1029
±10%	0.1716	0.1814	0.1569	0.1814	0.1912
±15%	0.2549	0.2696	0.2843	0.2500	0.3333
±20%	0.3284	0.3382	0.3922	0.3627	0.4412
±25%	0.4167	0.4559	0.4951	0.4510	0.5637
±30%	0.5098	0.5343	0.5588	0.5343	0.6716
±35%	0.6078	0.6520	0.6569	0.6422	0.8088
±40%	0.7010	0.7353	0.7402	0.7353	0.8529

TABLE III. DEFECT DEPTH ESTIMATION ACCURACY OF THE ANFIS MODEL FOR F25- F33 FEATURES WITH DIFFERENT ERROR-TOLEARNCE

Error-Tolerance	Input Parameters				
	F25	F26	F27	F28	F29
±1%	0.0049	0.0392	0.0098	0.0294	0.0098
±5%	0.0784	0.1569	0.0637	0.0931	0.0637
±10%	0.1716	0.3333	0.1373	0.1863	0.1520
±15%	0.3039	0.4853	0.2353	0.2941	0.2353
±20%	0.3578	0.6373	0.3137	0.4118	0.3235
±25%	0.4853	0.7059	0.4314	0.5441	0.4167
±30%	0.5441	0.7794	0.5098	0.6471	0.5000
±35%	0.6520	0.8971	0.6471	0.7010	0.6324
±40%	0.7402	0.9216	0.7353	0.8480	0.7304

Error-Tolerance	Input Parameters			
	F30	F31	F32	F33
±1%	0.0294	0.0196	0.0392	0.0098
±5%	0.1029	0.0882	0.1275	0.0686
±10%	0.1863	0.1814	0.2941	0.1912
±15%	0.3088	0.2549	0.4608	0.3088
±20%	0.4363	0.3529	0.5882	0.3627
±25%	0.5392	0.4265	0.7010	0.4706
±30%	0.6373	0.5147	0.8480	0.5637
±35%	0.6961	0.6176	0.8922	0.6863
±40%	0.8235	0.7206	0.9265	0.7402

D. Best Features-based ANFIS Model

The structure of the ANFIS model for the best seven features is depicted in Fig. 5. As shown in the figure, there are four Gaussian membership functions for each input feature. Fuzzy rules in the third layer combine the outputs of these membership functions by using the *AND* fuzzy operation. The shapes of the membership functions for the input features F1, F4 and F9 are described in Fig. 9, 10, and 11, respectively. For 100 epochs, the new ANFIS model is trained using the seven best features as an input pattern. The training performance error of the ANFIS model is calculated at 0.1482. Fig. 6 shows the model outputs against the training data. The x-axis represents the indices of the training data elements, whereas the y-axis represents the defect depths of the corresponding data elements. The 949 training data samples, representing the true defect depths, are plotted in blue. While the model outputs, representing the same defect depths estimated by the model, are plotted in red. Clearly, the model outputs (estimated defect depths) are satisfactory as they lie on or close to the true defect depths. Fig. 7 and 8 show the model outputs (plotted in red) against the 204-element testing data (plotted in blue) and 204-element checking data (plotted in blue), respectively. The testing and checking performance errors of the ANFIS model are calculated at 0.1410 and 0.1441, respectively. In both figures, the ANFIS model outputs (defect depth estimates) are close to the target outputs (true defect depths).

The four fuzzy rules obtained by the ANFIS model are shown in Fig. 9. The figure shows the output of the ANFIS model (defect depth estimated at 0.573) based on the values of the given input features: F1 = 0.02472; F4 = 0.01143; F9 = 0.0191; F10 = 0.01991; F11 = 0.06738; F14 = 0.0314; and F32 = -0.0318. The depth estimation accuracy for the seven-feature ANFIS model is demonstrated in Table IV. We can see that the overall estimation accuracy has improved for all levels of error-tolerance. Particularly for the error-tolerance levels ±10%, ±15%, and ±20%, the estimation accuracies achieved are, respectively, 61%, 74%, and 87%, which are way higher than any accuracy obtained by a single feature.

E. Feature Selection for ANFIS-Models

In this section the weight-correlation method is used to assign weights for each feature. Features with the highest weights are then selected to train a new ANFIS model. This method produces different sets of features, ranging from 16 to 29 features. The ANFIS model is examined with ever produced feature set. The results are reported in Table V. As shown in the table, using 22 features as an input vector to the ANFIS model yields the best overall depth estimation accuracies. This is especially true for the error-tolerance levels ±15%, ±20%, ±25%, ±30%, ±35%, and ±40%, where the ANFIS models defect depth estimation accuracies achieved are 80.39%, 87.75%, 91.18%, 95.59%, 97.06%, and 98.04%, respectively. Only, using all the 29 features can give comparable results.

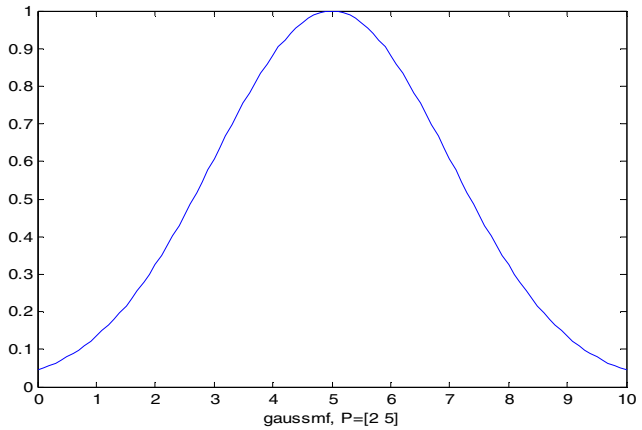

Fig. 4. Gaussian membership function with standard deviation = 2 and mean = 5

978-1-4673-7606-8/15/$31.00 ©2015 IEEE

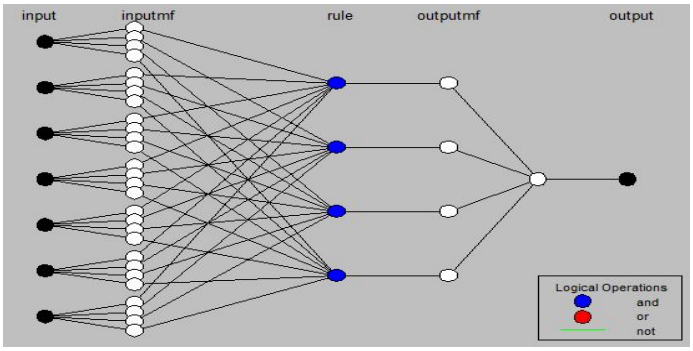

Fig. 5. ANFIS structure for the selected seven featues (F1, F4, F9, F10, F11, F14, F32)

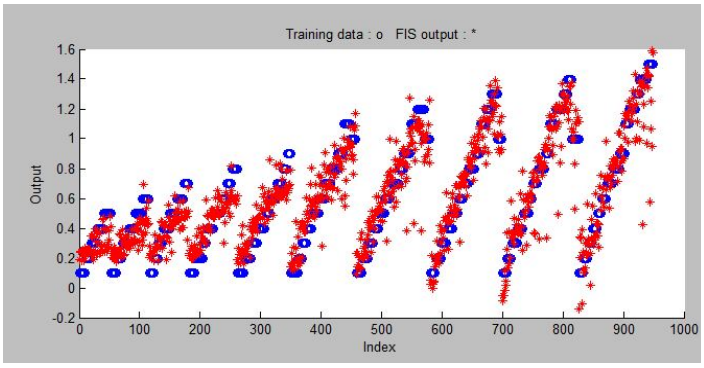

Fig. 6. The outputs of the ANFIS model (red) against the training data (blue)

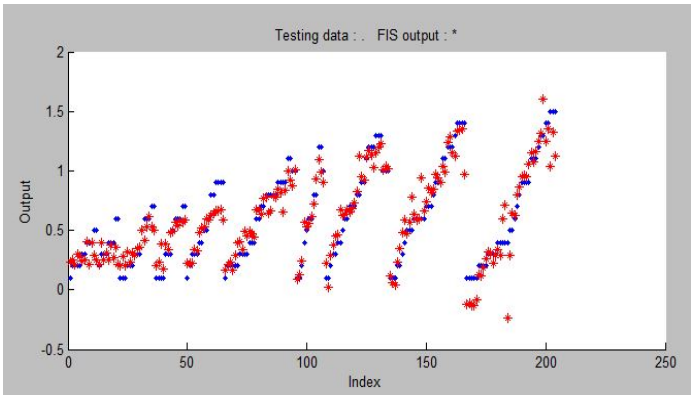

Fig. 7. The outputs of the ANFIS model (red) against the testing data (blue)

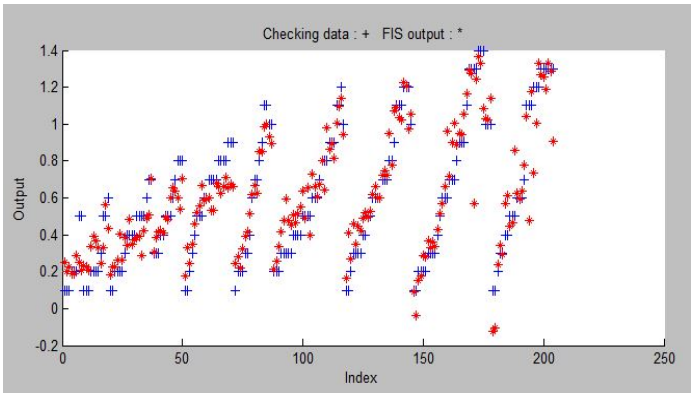

Fig. 8. The outputs of the ANFIS model (red) against the checking data (blue)

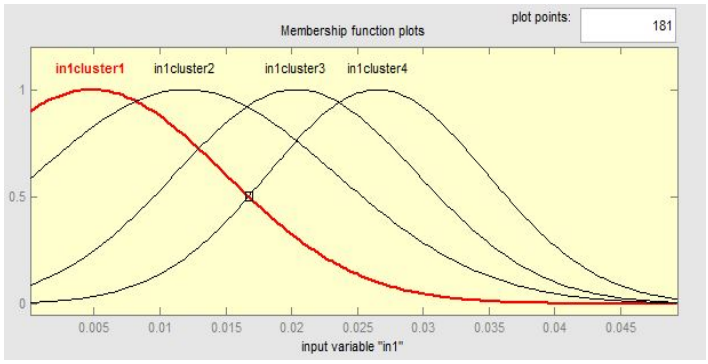

Fig. 9. Fuzzy membership function for F1

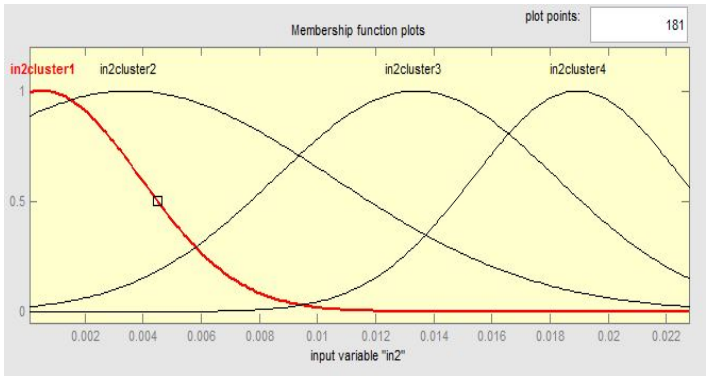

Fig. 10. Fuzzy membership function for feature F4

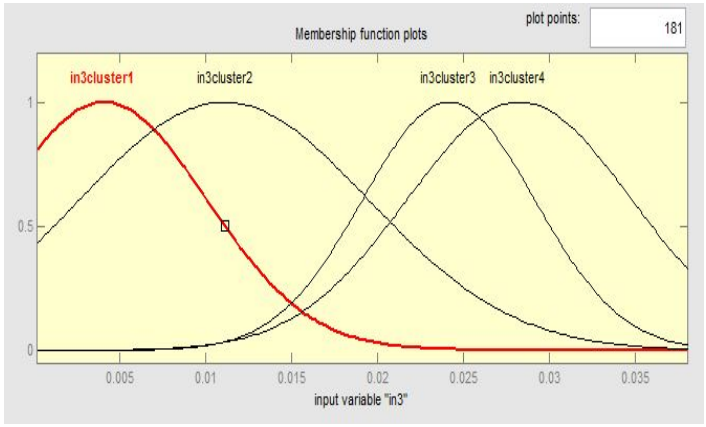

Fig. 11. Fuzzy membership function for feature F9

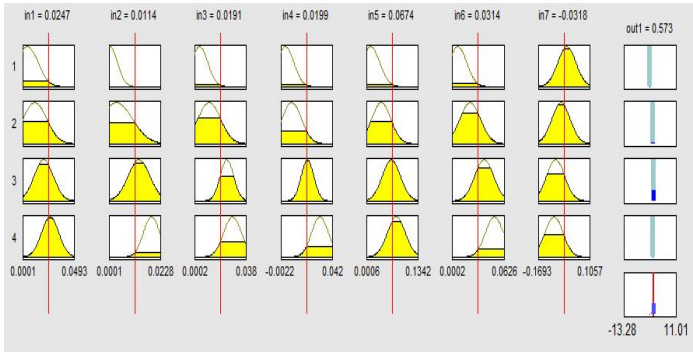

Fig. 12. The four fuzzy rules of the ANFIS model for the features F1, F4, F9, F10, F11, F14, and F32

978-1-4673-7606-8/15/$31.00 ©2015 IEEE

TABLE IV. DEFECT ESTIMATION ACCURACY OF THE ANFIS MODEL FOR THE SEVEN FEATURES F1-F4-F9-F10-F11-F14-F32 WITH DIFFERENT ERROR-TOLEARNCES

Error-Tolerance	Input Features (F1 F4 F9 F10 F11 F14 F32)
±1%	0.0637
±5%	0.3529
±10%	0.6127
±15%	0.7402
±20%	0.8725
±25%	0.9314
±30%	0.9510
±35%	0.9755
±40%	0.9853

TABLE V. DEFECT DEPTH ESTIMATION ACCURACY OF THE ANFIS MODEL FOR VARIOUS COMBINATIONS OF FEATRUES WITH DIFFERENT ERROR-TOLEARNCES

Error-Tolerance	Input Parameters				
	16	17	18	19	20
±1%	0.0637	0.0637	0.0392	0.0343	0.0686
±5%	0.2843	0.3235	0.3137	0.3382	0.2598
±10%	0.6225	0.5686	0.5980	0.5441	0.5245
±15%	0.7647	0.7255	0.7647	0.7500	0.7451
±20%	0.8431	0.8725	0.8627	0.8333	0.8529
±25%	0.8922	0.9216	0.9020	0.8922	0.8971
±30%	0.9167	0.9461	0.9363	0.9363	0.9167
±35%	0.9412	0.9608	0.9510	0.9608	0.9314
±40%	0.9608	0.9657	0.9706	0.9657	0.9608

Error-Tolerance	Input Parameters				
	21	22	23	24	25
±1%	0.0539	0.0637	0.0637	0.0588	0.0588
±5%	0.2941	0.3529	0.3480	0.3235	0.3775
±10%	0.5441	0.6225	0.5784	0.6176	0.5980
±15%	0.7451	0.8039	0.7647	0.7941	0.7843
±20%	0.8676	0.8775	0.8578	0.8676	0.8382
±25%	0.8971	0.9118	0.9167	0.9216	0.9069
±30%	0.9216	0.9559	0.9363	0.9412	0.9510
±35%	0.9461	0.9706	0.9412	0.9461	0.9608
±40%	0.9657	0.9804	0.9608	0.9657	0.9804

Error-Tolerance	Input Parameters			
	26	27	28	29
±1%	0.0686	0.0637	0.0441	0.0588
±5%	0.3137	0.3725	0.3284	0.3627
±10%	0.5980	0.5931	0.6127	0.6324
±15%	0.7696	0.7647	0.7843	0.7990
±20%	0.8431	0.8578	0.8824	0.8529
±25%	0.9020	0.9020	0.9069	0.8971
±30%	0.9412	0.9363	0.9363	0.9314
±35%	0.9657	0.9510	0.9657	0.9510
±40%	0.9804	0.9657	0.9706	0.9608

V. CONCLUSION

Estimating metal-loss defect depths in oil and gas pipeline is a pre-requisite step in determining the defect severity, based on which urgent and preventative measures can be carried out. Pipeline monitoring systems usually utilize Magnetic Flux Leakage (MFL) sensors that scan the metal pipelines and collect defect-related data. In this paper, a new adaptive neuro-fuzzy inference system (ANFIS)-based approach for defect depth estimation is proposed. Meaningful features are first extracted from MFL signals and fed to the proposed ANFIS model. A hybrid learning algorithm is adopted in the training stage. The proposed approach is tested for different levels of error-tolerance. At the levels of ±15%, ±20%, ±25%, ±30%, ±35%, and ±40%, the best defect depth estimates obtained by the new approach are 80.39%, 87.75%, 91.18%, 95.59%, 97.06%, and 98.04%, respectively. As future work, we intend to extract more sophisticated features to enhance the defect depth estimation accuracies. Moreover, new techniques will be explored to determine defect lengths, which along with defect depth, can be used to determine the overall defect severity.

ACKNOWLEDGMENT

This work was made possible by NPRP grant # [5-813-1-134] from Qatar Research Fund (a member of Qatar Foundation). The findings achieved herein are solely the responsibility of the authors.

REFERENCES

[1] P. Nicholson, "Combined CIPS and DCVG survey for more accurate ECDS data," Journal of World Pipelines, vol. 7, pp. 1-7, 2007.

[2] S. K. Sinha and M. D. Pandey, "Probabilistic neural network for reliability assessment of oil and gas pipelines," Computer-Aided Civil and Infrastructure Engineering, vol. 17(5), pp. 320-329, 2002.

[3] S. K. Sinha and F. Karray, "Classification of underground pipe scanned images using feature extraction and neuro-fuzzy algorithm," IEEE Transactions on Neural Networks, vol. 13(2), pp. 393-401, 2002.

[4] A. A. Carvalho, et al, "MFL signals and artificial neural networks applied to detection and classification of pipe weld defects," Ndt & E International, vol. 39(8), pp. 661-667, 2006.

[5] M. Zhongli and H. Liu, "Pipeline defect detection and sizing based on MFL data using immune RBF neural networks," IEEE Congress on Evolutionary Computation, pp. 3399-3403, 2007.

[6] J. R. Jang, "ANFIS: Adaptive-network-based fuzzy inference system," IEEE Transactions on Systems, MAN, and Cybernetics, vol. 23, pp. 665-685, 1993.

[7] K. Mandal and D. L. Atherton, "A study of magnetic flux-leakage signals," Journal of Physics D: Applied Physics, vol. 31(22), pp. 3211, 1998.

[8] I. Daubechies, Ten Lectures on Wavelets. SIAM: Society for Industrial and Applied Mathematics, 1992.

[9] S. Mallat, A Wavelet Tour of Signal Processing. Academic Press, 2008.

[10] M. Misiti, Y. Misiti, G. Oppenheim, and J. M. Poggi, Wavelets and their Applications. Wiley-ISTE, 2007.

[11] J. N. Bradley, C. M. Brislawn, and T. Hopper, "FBI wavelet/scalar quantization standard for gray-scale fingerprint image compression," In: SPIE Procs, Visual Information Processing II, vol. 1961, pp. 293–304, 1993.

[12] M. Unser and A. Aldroubi, "A review of wavelets in biomedical applications," Proceedings of the IEEE, vol. 84 (4), pp. 626–638, 1996.

[13] S. Shou-peng and Q. Pei-wen, "Wavelet based noise suppression technique and its application to ultrasonic flaw detection," Ultrasonics, vol. 44(2), pp. 188-193, 2006.

[14] A. Muhammad and Satish Udpa, "Advanced signal processing of magnetic flux leakage data obtained from seamless gas pipeline," Ndt & E International, vol. 35(7), pp. 449-457, 2002.

[15] S. Mukhopadhyay and G. P. Srivastava, "Characterisation of metal loss defects from magnetic flux leakage signals with discrete wavelet transform." Ndt & E International, vol. 33(1), pp. 57-65, 2000.

[16] K. Hwang, et al, "Characterization of gas pipeline inspection signals using wavelet basis function neural networks," NDT & E International, vol. 33(8), pp. 531-545, 2000.

[17] N. Roohollah, S. Safavi, and S. Shahrokni, "A reduced-order adaptive neuro-fuzzy inference system model as a software sensor for rapid estimation of five-day biochemical oxygen demand," Journal of Hydrology, vol. 495, pp. 175-185, 2013.

978-1-4673-7606-8/15/$31.00 ©2015 IEEE

[18] K. Mucsi, K. Ata, and A. Mojtaba, "An Adaptive Neuro-Fuzzy Inference System for estimating the number of vehicles for queue management at signalized intersections," Transportation Research Part C: Emerging Technologies, vol. 19(6), pp. 1033-1047, 2011.

[19] A. Zadeh, et al, "An emotional learning-neuro-fuzzy inference approach for optimum training and forecasting of gas consumption estimation models with cognitive data," Technological Forecasting and Social Change, vol. 91, pp. 47-63, 2015.

[20] H. Azamathulla, A. Ab Ghani, and S. Yen Fei, "ANFIS-based approach for predicting sediment transport in clean sewer," Applied Soft Computing, vol. 12(3), pp. 1227-1230, 2012.

[21] A. Khodayari, et al, "ANFIS based modeling and prediction car following behavior in real traffic flow based on instantaneous reaction delay," IEEE Intelligent Transportation Systems Conference, pp. 599-604, 2010.

[22] A. Kulaksiz, "ANFIS-based estimation of PV module equivalent parameters: application to a stand-alone PV system with MPPT controller," Turkish Journal of Electrical Engineering and Computer Science, vol. 21(2), pp. 2127-2140, 2013.

[23] D. Petković, et al, "Adaptive neuro-fuzzy estimation of conductive silicone rubber mechanical properties," Expert Systems with Applications, vol. 39(10), pp. 9477-9482, 2012.

[24] M. Chen, "A hybrid ANFIS model for business failure prediction utilizing particle swarm optimization and subtractive clustering," Information Sciences, vol. 220, pp. 180-195, 2013.

[25] M. Iphar, "ANN and ANFIS performance prediction models for hydraulic impact hammers," Tunnelling and Underground Space Technology, vol. 27(1), pp. 23-29, 2012.

978-1-4673-7606-8/15/$31.00 ©2015 IEEE